ICSV19
Vilnius, Lithuania
July 08-12, 2012

# LINEAR AND NONLINEAR DYNAMICS OF A CIRCULAR CYLINDRICAL SHELL UNDER STATIC AND PERIODIC AXIAL LOAD

Antonio Zippo, Marco Barbieri, Matteo Strozzi, Vito Errede and Francesco Pellicano

*Dipartimento di Ingegneria Meccanica e Civile, Universitá di Modena e Reggio Emilia*
*Modena, Italy, 41125*
*e-mail: francesco.pellicano@unimore.it*

In this paper an experimental study on circular cylindrical shells subjected to axial compressive and periodic loads is presented. The setting of the experiment is explained and deeply described along with a complete analysis of the results. The linear and the nonlinear dynamic behaviour associated with a combined effect of compressive static and a periodic axial load has been considered and a chaotic response of the structure has been observed close to the resonance. The linear shell behaviour is also investigated by means of a theoretical and finite element model, in order to enhance the comprehension of experimental results, i.e. the natural frequencies of the system and their ratios.

## 1. Introduction

Circular cylindrical shells are important elements in many Engineering fields e.g. Aerospace, Nuclear, Civil and the need of more and more efficient structures in terms of strength and weight led to a strong reduction of safe factors; one of the direct consequences of weight reduction is the increasing of vibration problems. Nowadays, several commercial softwares allow to carry out static, stability and vibration analyses; however, regarding the shell dynamics, such kind of analyses are generally reliable in the linear field only. Difficulties in developing accurate models for shell structures were the motivations of a large scientific production, withal there are few experimental studies about dynamic instabilities and the comparisons between theory and experiments are not yet satisfactory. The fundamental investigation on the stability of circular cylindrical shells is due to Von Karman and Tsien [1] that analyzed the static stability (buckling) and the postcritical behavior of axially loaded shells. In this study, it was clarified that the discrepancies between forecasts of linear models and experimental results were due to the intrinsic simplifications of linear models; indeed, linear analyses are not able to predict the actual buckling phenomenon observed in experiments. Vijayaraghavan and Evan-Iwanowski [2] analyzed, both analytically and experimentally, the parametric instabilities of a circular shell under seismic excitation. The cylinder position was vertical and the base was axially excited using a shaker. Instability regions are found analytically and compared to experimental results. The Donnells nonlinear shallow-shell theory [3] was used by Gonalves and Del Prado [4] to analyze the dynamic buckling of a perfect circular cylindrical shell under axial static and dynamic loads. Pellicano and Avramov [5] published a paper concerning the nonlinear dynamics of a shell with base excitation and a top disk. The work was mainly theoretical and only some experimental

Table 1: Natural frequencies of mode (1,4) at increasing preload.

| Preload ($N$) | Natural Frequency (FEM) ($Hz$) | Natural Frequency (Experimental) ($Hz$) | relative error ($\%$) |
|---|---|---|---|
| 0 | 1623 | 1621 | 0.1 |
| 50 | 1619 | 1614 | 0.3 |
| 100 | 1616 | 1610 | 0.4 |
| 150 | 1612 | 1604 | 0.5 |
| 200 | 1608 | 1598 | 0.6 |
| 250 | 1604 | 1592 | 0.7 |

results concerning the linear dynamics were presented. The shell was modeled using the nonlinear Sanders Koiter theory [3] and a reduced order model was used. Kubenko and Kovalchuk [6] published an experimental work focused on shells made of composite materials; they pointed out the inadequateness of the linear viscous damping models. Axial loads (base excitation, and free top end of the shell) as well as combined loads were considered. Dynamic instability regions were determined experimentally: a disagreement between previous theoretical models (narrower region) and experiments (wider) was found, the conjecture made by such scientists was that the disagreement was due to shells geometric imperfections. Such paper summarizes some of experimental results published on a previous book (Kubenko et al.) [7] (see e.g. page 123, figure 2.23 gives an interpretation of the enlargement of instability boundaries)

In the present paper, circular cylindrical shells subjected to axial loads having static (compressive) and harmonic components are investigated.

## 2. Finite element analysis

Finite Element modal analysis has been carried out for each step of the applied preload. Mode shape description for a generic mode (m,n) [8] is characterized with an own mode shape where:

$m$ number of longitudinal half-waves (m = 1,2,3,..)

$n$ number of circumferential waves (n = 1,2,3,..)

In Figure 1 the modal shape of mode (1,4) is shown. In Table 1 a comparison between numerical and experimental frequency for mode (1,4) is shown.

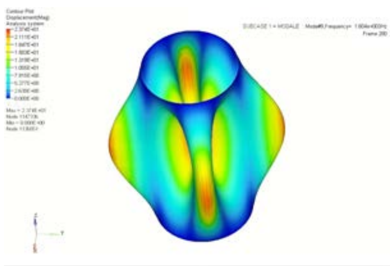

Figure 1: F.E.M. analysis, mode (1,4)

## 3. Experiments

This section provides informations about the experimental setup developed to test thin shell structures under constant axial load and periodical excitation. In Figure 2 a schematic representation of the setup is shown. A shaker is rigidly inserted in a frame designed for the application of the preload. Connections to the system for data acquisition are shown.

### 3.1 Description

The system under investigation consists of a circular cylindrical shell, made of aluminum alloy, clamped both base and top sides by means of two worm gear clamps at two rigid supports. The bottom support is an aluminum alloy circular disk rigidly bolted to the shaker. The top disk is connected to the frame by means of a dynamic load cell, a stinger, and a static load cell. The stinger is introduced in order to reduce the effects of misalignments. A laser vibrometer is used to measure the velocity of the side of the shell and its output is routed both to the spectrum analyzer and to the LDS controller. The control system is open-loop in order to avoid control instabilities induced by nonlinear behavior of the tested structures.

The characteristics of the shell are the following: length $L = 0.137m$, thickness $h = 0.1 \times 10^{-3}m$, mean radius $R = 32.9 \times 10^{-3}m$, density $\rho = 2796\frac{kg}{m^3}$, Young's modulus $E = 71.020 \times 10^9\frac{N}{m^2}$ , Poisson's ratio$\nu = 0.31$ and static preload $P_0 = 0 - 250N$.

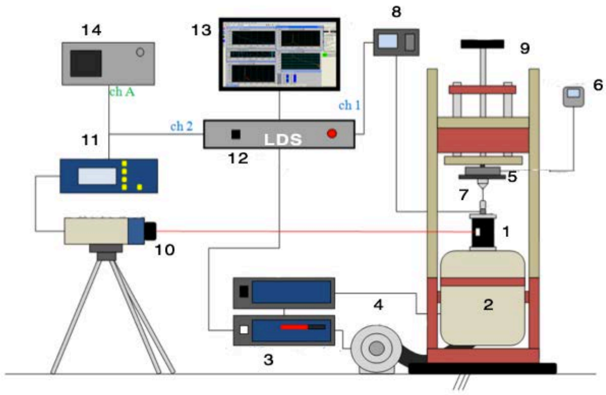


Figure 2: System setup: (1) structure under test (2) shaker (3) shaker amplifier (4) air cool system (5) static load cell (6) digital load gauge (7) force transducer pcb m231b (8) force transducer amplifier (9) press system to apply static preload (10) laser vibrometer (11)laser controller (12) lds dactron laser usb shaker control system (13) pc (14) spectrum analyzer ono-sokki cf-5220.

The press system has been suitably designed for this research. A screw can move up or down a plate which applies the desired preload to the shell, both compressive and tractive. A static load cell AEP transducers TC8 10KN" is interfaced with a digital load gauge that displays the exact preload applied to the shell. The Shaker LDS V530 is integrated rigidly in the press system structure, is powered independently and equipped with a system of air cooling.

The laser vibrometer is targeted on the shell surface and plays a significant role as it measures velocity data acquisition on the shell side without interfering with it. This point is very significant for thin structures, because the use of a standard accelerometer would introduce an undesired extra mass, thus altering the symmetry of the structure. The signal coming from the laser is splitted and directed both to the spectrum analyzer, used to detect the regions of instability, and to the LDS controller.

### 3.2 Data Presentation

In this section all tests carried out on the shell are described. Formerly a few tests were done to calibrate the devices properly, then several combination were investigated for different preloads. The experimental analysis was carried out by sweeping frequencies from 700Hz to 2500Hz, with a step rate of 7.5 Hz per second, starting from the highest frequency (2500Hz) towards the lower frequency (700Hz) and backwards, each time varying the magnitude of the oscillations generated from the shaker, from 0.1 V with regular steps of 0.1 V up to the maximum value of 1.0 V. These sweeps were repeated, not only by varying the power supplied to the shaker, but also by imposing an increasing axial static compressive load $P_0$. The static axial load is increased from $0N$ up to $250N$ (safety limit to avoid shaker damage). Results are presented for preload values of $0N$, $100N$ and $250N$ and for voltage levels of $0.5V$ and $0.8V$. In Figures 3 and 4, d and u represent the decreasing frequency sweep (d, down) and the increasing frequency sweep (u, up).

### 3.2.1 External Load Amplitude of 0.5 volt

In Figure 3 the dynamic axial load vs frequency is plotted whereas in figure 4 the amplitude of vibration of the shell (in terms of velocity) vs.-frequency are shown.

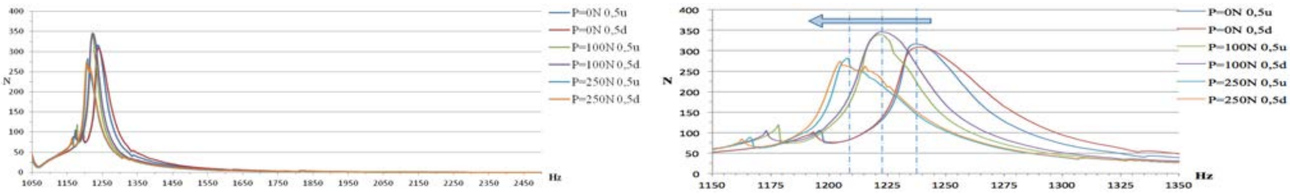


(a) (b)

Figure 3: Dynamic load-frequency diagram for different preloads at 0.5 volt.

Dynamic load-frequency diagrams show a reduction in terms of resonance frequency for increasing preloads. The amplitude of the resonance peak has a peculiar behavior: it has a maximum value of 350N for the mid value of preload (100N), see Figure 3b. This point needs further investigations. The same behavior can be observed in terms of velocity amplitude at the target point, see Figure 4. The maximum velocity, i.e. the maximum amplitude of vibration, is seen for $P_0 = 100N$. The velocity frequency diagram shows another resonance between 1300 and 1350 Hz. For this resonance, the amplitude of vibration is minimum for $P_0 = 100N$.

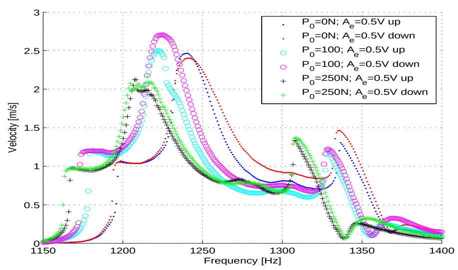


Figure 4: Amplitude-frequency diagram for different preloads at 0.5 volt.

### 3.2.2 External Load Amplitude of 0.8 volt

Figure 5 and 6 present the corresponding experimental results for 0.8V excitation amplitude. From Figure 5a and 5b it is noted that increasing the static load $P_0$, the maximum peak in dynamic load is reduced. The system presents the opposite behavior with respect to the case of 0.5V excitation. Moreover, Figure 6 shows again the frequency reduction due to the preload.

## 4. Measured non linear phenomena

The behavior of the structure close to the mode (1,4) is investigated. Numerical and experimental analyses show that this mode is close to 1623 Hz (see Table 1) and it is quite far from other modes. The amplitude-frequency diagram for such resonance is shown in Figure 7. In order to describe the nonlinear behavior close to the resonance, it is useful to introduce the following dimensionless values:

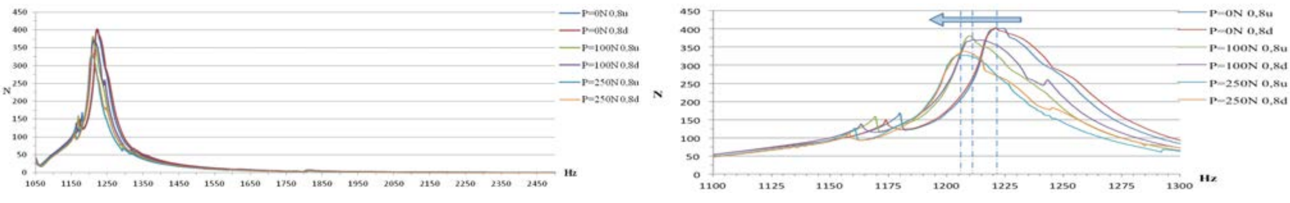


(a) (b)

Figure 5: Dynamic load-frequency diagram for different preloads at 0.8 volt.

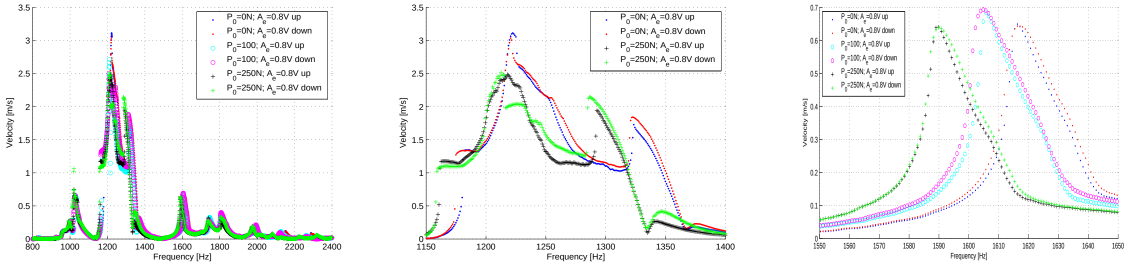


(a) (b) (c)

Figure 6: Amplitude-frequency diagram for different preloads at 0.8 volt.

1. $\omega_x = \omega_n / \omega_{0,1}$ , is the ratio between the frequency corresponding to the maximum amplitude for the n-th excitation amplitude and the frequency at which the maximum occurs for the reference case (0.1 V);

2. $v_x = v_n / v_{0,1}$ , is the ratio between the corresponding maximum velocities.

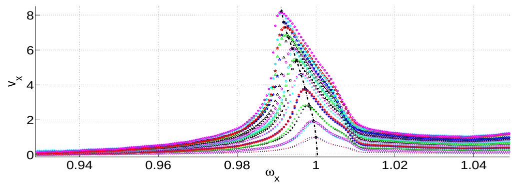


Figure 7: Amplitude-frequency diagram. mode (1,4); $P_0 = 100N$; voltage levels 0.1-1V

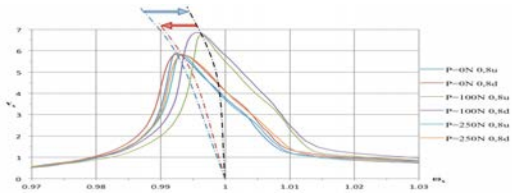

Figure 8: Amplitude-frequency diagram comparison of mode (1,4) with different preloads (0N, 100N and 250N) at 0.8 volt

In terms of dimensionless variables, the backbone can be drawn by interpolating the maxima, Figure 7 it results that the shell presents a softening behavior. The backbone curve moves to the left with respect to the vertical line through the resonance frequency.

Figure 8 shows dependence of the non linear behavior on the different values of the preload. The preload of $100N$ produces a less softening resonance, with respect to the non preloaded case and the case of $250N$ preload.

## 5. Nonstationary response

Tests performed on the shell structure pointed out the existence of certain frequency intervals characterized by high amplitude of vibration and complex dynamics; in the following we will call them ”instability regions”, this gives the clear idea that the periodic orbit has lost stability. Table 2 summarizes the instability ranges found during experiments and Figures 9 - 12 shows the time histories and spectra of the lateral shell vibration at different forcing loads and with a static compression of $100N$.

Table 2: Frequency ranges of instability regions with different preload.

| $P_0$ $(N)$ | Voltage level $(V)$ | Instability range $(Hz)$ |
|---|---|---|
| | 0.8 | 1210.01 - 1217.92 |
| 100 | 0.9 | 1205.61 - 1218.80 |
| | 1.0 | 1201.22 - 1225.84 |
| | 0.7 | 1208.25 - 1210.01 |
| 150 | 0.8 | 1202.97 - 1212.53 |
| | 0.9 | 1199.46 - 1215.29 |
| | 1.0 | 1196.82 - 1221.44 |
| | 0.7 | 1209.13 - 1211.77 |
| 200 | 0.8 | 1207.37 - 1213.53 |
| | 0.9 | 1195.06 - 1215.29 |
| | 1.0 | 1191.54 - 1218.80 |
| | 0.5 | 1208.25 - 1215.29 |
| 250 | 0.6 | 1204.73 - 1221.44 |
| | 0.7 | 1202.92 - 1234.63 |
| | 0.8 | 1198.53 - 1236.39 |
| | 0.9 | 1194.18 - 1238.42 |
| | 1.0 | 1189.78 - 1242.42 |

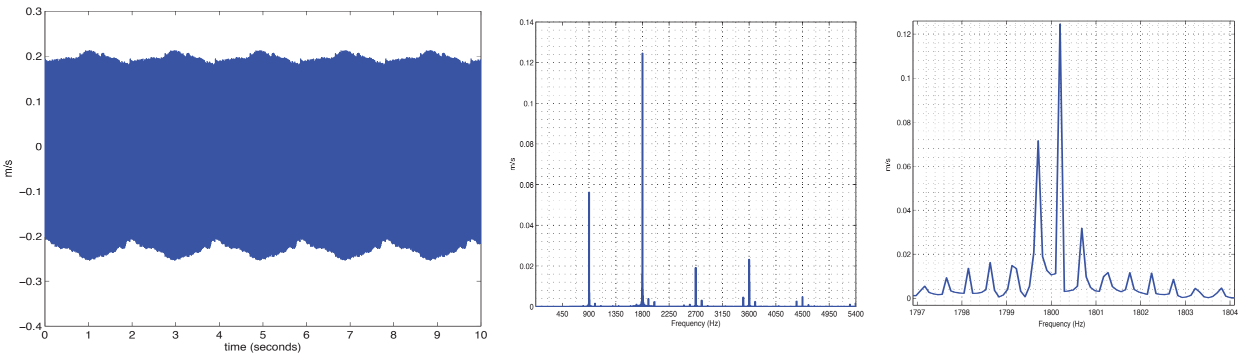


Figure 9: Time history and Spectrum at 900 Hz forcing load

In Figure 9 the dynamic scenario is represented, the excitation frequency is $900Hz$. The response is quasi-periodic, i.e. there is an amplitude modulation that presents two time scales: i) a slow time scale with period of 2s (see $0.5Hz$ sidebands); ii) intermediate time scale with period of 10-2s (see $100Hz$ sidebands). The response is dominated by the second main spectral harmonics ($1800Hz$), suggesting an important role of quadratic nonlinearities; this role is also confirmed by the loosing of symmetry in the time response ($max = 0.2m/s$, $min = -0.25m/s$).

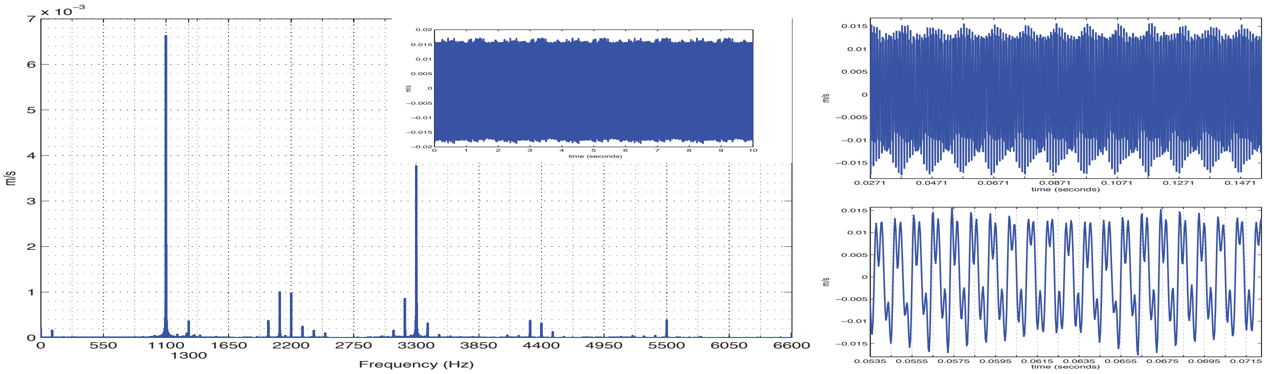


Figure 10: Time history and Spectrum at 1100 Hz forcing load

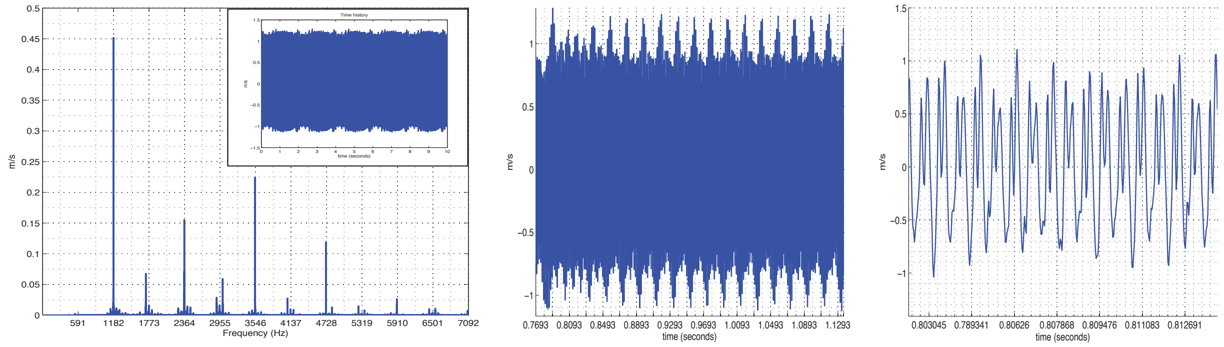


Figure 11: Time history and Spectrum at 1182 Hz forcing load

At $1100 Hz$ (Figure 10) the scenario changes; here the energy in frequency domain is mainly concentrated at 1100 and $3300 Hz$. This means that here the linear and cubic behaviors are dominant; note that this is confirmed by the symmetry in the time history.

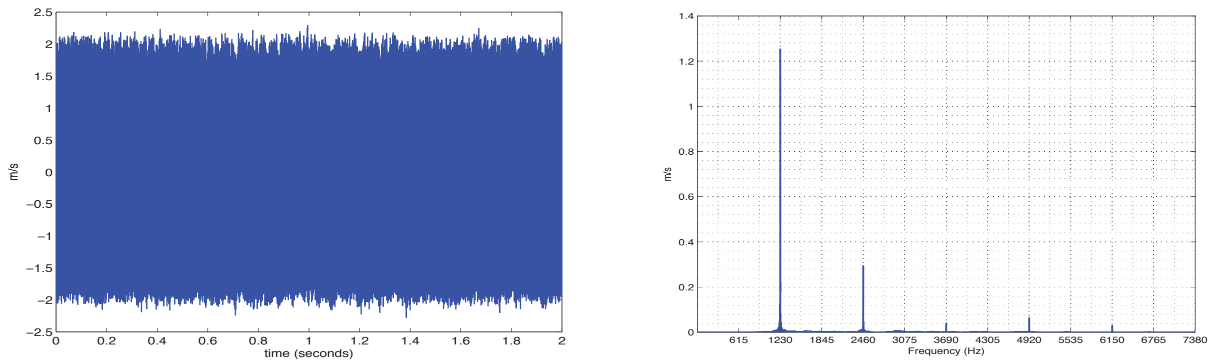


Figure 12: Time history and Spectrum at 1230 Hz forcing load

At $1182 Hz$ (Figure 11) an interesting phenomenon takes place, the response is quasi-periodic but something interesting happens in the periodicity. The main spikes in the spectrum are spaced of about $590 Hz$, i.e. one half the excitation frequency. This means that the periodic part of the response presents a fundamental frequency of $590 Hz$. The straightforward consideration is that the response is one half sub-harmonic; this is partially contradicted by the spectrum that does not present spikes at $590 Hz$. However, if one zooms around $590 Hz$, then will disclose an extremely small peak. Our conjecture is that the response is sub-harmonic and the amplitude of the fundamental harmonic is negligible.

## 6. Conclusions

The dynamic behavior of a thin cylindrical shell under static axial preload and harmonic external axial load has been characterized. An *ad hoc* setup has been developed in order to measure both the dynamic load and the amplitude of vibration on the shell surface. Tests performed at different preload values and different amplitudes of the external excitation pointed out the existence of non linear behavior in certain instability ranges. Chaos is found close to 1230 Hz and a very well defined softening behavior can be observed close to the mode (1,4). Non linear dependence of the response on the preload parameter is observed. Further experiments and correlation with numerical and theoretical models need to be performed in order to fully understand the observed phenomena.

## REFERENCES

[1] Von Kármán, T., and Tsien, H., 1941. "The buckling of thin cylindrical shells under axial compression". *Journal of the Aeronautical Sciences,* ***8***(8), pp. 303–312.

[2] Vijayaraghavan, A., and Evan-Iwanowski, R. M., 1967. "Parametric instability of circular cylindrical shells". *Journal of Applied Mechanics,* ***34***(4), pp. 985–990.

[3] Amabili, M., 2008. *Nonlinear Vibrations and Stability of Shells and Plates*. Cambridge University Press.

[4] Gonçalves, P. B., and Del Prado, Z. J., 2002. "Nonlinear oscillations and stability of parametrically excited cylindrical shells". *Meccanica,* ***37***, pp. 569–597.

[5] Pellicano, F., and Avramov, K., 2007. "Linear and nonlinear dynamics of a circular cylindrical shell connected to a rigid disk". *Communications in Nonlinear Science and Numerical Simulation,* ***12***(4), pp. 496 – 518.

[6] Kubenko, V., and Koval'chuk, P., 2009. "Experimental studies of the vibrations and dynamic stability of laminated composite shells". *International Applied Mechanics,* ***45***, pp. 514–533. 10.1007/s10778-009-0209-4.

[7] Kubenko, V. D., Koval'chuck, P. S., and Krasnopol'skaya, T. S., 1984. *Nonlinear interaction of the flexural modes of vibration of cylindrical shells*. Nauk. Dumka.

[8] Leissa, A. W., 1973. *Vibration of shells*. NASA SP-288, Scientific and Technical Information Office, National Aeronautics and Space Administration; Washington, DC.